

Electron-stimulated desorption total-removal cross sections for H₂ and HD monolayers physisorbed on graphite

Bin Xia and S. C. Fain, Jr.*

Department of Physics, University of Washington, Seattle, Washington 98195

(Received 25 April 1994; revised manuscript received 5 July 1994)

The decay in time of the number of positive ions desorbed by 62-eV electrons incident on H₂ and HD submonolayers physisorbed on graphite is used to measure the electron-stimulated desorption (ESD) total-removal cross sections. The nonexponential decay is analyzed by approximating the electron-beam spatial profile as a Gaussian. The total removal rate is found to be linear in electron current density. The total ESD removal cross sections deduced at 62 eV are much larger than the gas-phase total-ionization cross section of 0.01 nm²: 1.2 nm² for HD and 5.2 nm² for H₂, with a 20% uncertainty.

INTRODUCTION

Quantitative measurements of total electron-stimulated desorption (ESD) from physisorbed monolayers have included Xe, Kr, and Ar on Ag(111);¹ Xe and Kr on W(110);²⁻⁴ N₂O, Ar, and Kr on Ru(001)^{5,6} and O₂ on top of a chemisorbed O monolayer.⁷ Ionization has been proposed as the initial step of one ESD process; the excited molecule finds itself in an unstable position and picks up kinetic energy either by being accelerated to a new equilibrium position⁸ or by wave-packet squeezing.⁹ Electron induced dissociation can cause desorption directly as well as by knocking other molecules off the surface.⁷ For the weakly bound H₂, HD, and D₂ on graphite, phonons excited in the substrate by the incident electrons provide an additional desorption mechanism, as will be discussed below.

A separate paper¹⁰ reports the angle, mass, and energy distributions for positive ions desorbed by electrons from H₂, HD, and D₂ monolayers physisorbed on graphite. In this paper, we use the number of positive ions to infer the decay in coverage with time for various electron current densities after the gas flux to the sample is stopped. The ESD total-removal cross sections for HD (H₂) are found to be approximately 1.2 (5.2) nm² for 62-eV electrons incident on submonolayers in the coverage regime where the equilibrium state is commensurate solid islands coexisting with a low-density two-dimensional vapor.¹¹ The results are so much larger than the gas-phase total-ionization cross section¹² of 0.01 nm² at 62 eV that substrate excitations are likely to be quite important.

The apparatus is described in Ref. 10. The electron beam current density $J_e(r)$ measured with the beam profile device described in Ref. 10 could be approximated by a Gaussian

$$J_e(r) = J_0 \exp(-r^2/a^2). \quad (1)$$

The Gaussian width of the beam at the lowest currents used was $a = 0.64 \pm 0.05$ mm (giving a full width at half maximum of 1.1 mm). The minimum pulse width of $W = 0.15$ μ s and repetition rate of 50 kHz gave an average measured current I of 0.48 nA and thus a current density of $J_0 = I/(\pi a^2) = 0.038$ μ A/cm². The electron energy at the sample was 62 eV, the sample bias was

$V_S = +8$ V, and the retarding grid bias was $V_G = 0$ V. For ESD measurements from HD, the pulse width W was changed keeping the repetition rate at 50 kHz; for H₂, the pulse length was fixed at $W = 0.15$ μ s and the repetition rate was increased. By varying the pulse duty cycle to vary the average current, changes in the electron-beam width and position were minimized at the lower duty cycles. At the highest duty cycle used for HD, the beam width was $a = 0.77 \pm 0.05$ mm.

For each series of measurements, the substrate was dosed for a fixed time with a given flux. The total dose was adjusted to produce a coverage less than a completed commensurate monolayer (6×10^{14} molecules/cm²). After each measurement, the substrate was warmed to about 50 K to remove physisorbed impurities.

TIME-DEPENDENT ESD OF HD AND H₂

Figure 1 shows examples of adsorption-desorption measurements made by counting the total number of ions desorbed from the adsorbate. Within minutes after the crystal was cooled to 6 or 7 K a flux of gas was turned on [at $t = -260$ s for HD in Fig. 1(a) and $t = -190$ s for H₂ in Fig. 1(b)]. The electron gun pulses were turned on for 1 to 2 s at a time to sample the coverage during the adsorption process. (The scatter in counts during adsorption is due to either the gun being on for less than a complete counting interval or to removal of coverage.) The nonlinearity with time just at the start of dosing could be due to a strong dependence on coverage of the sticking probability for the first molecules striking the surface.¹³ We attribute the linearity with time during dosing to a sticking coefficient and an ion yield that are approximately constant in this coverage range. Before a steady-state coverage was reached, the gas flux was rapidly reduced to zero and the electron gun pulses were turned on continuously. For removal rates by the electron beam significantly greater than any readsorption of gas from the residual background, the reduced ion counts are dominated by the electron-beam removal. The rate of drop in local pressure after the flux was reduced to zero was estimated by using the same flux of HD for the same time with the sample at room temperature. Within 3 s after the gas flux was shut off, the HD signal at a mass spectrometer remote from the sample dropped to 1/20 of its

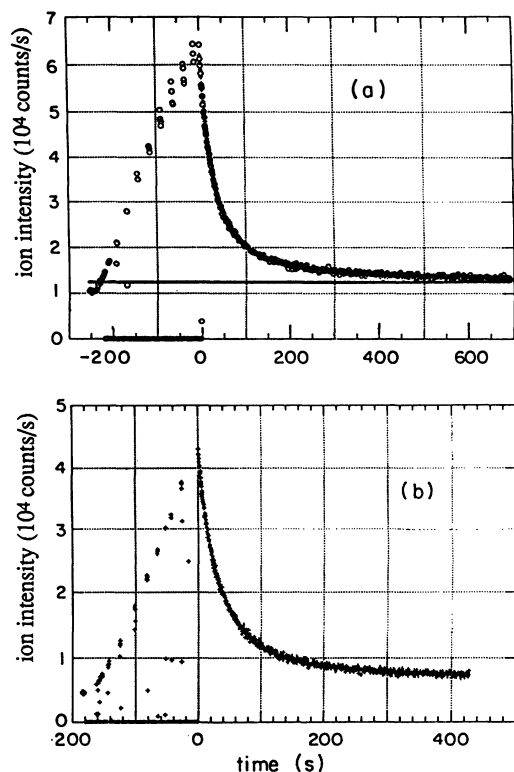


FIG. 1. Adsorption-desorption measurement for (a) HD and (b) H_2 physisorbed on graphite. The electron beam was turned on for 1 to 2 s at a time to measure the coverage up to $t=0$. Then the gas flux was shut off and the beam was left on with an average current density of (a) $0.77 \mu A/cm^2$ and (b) $0.17 \mu A/cm^2$. Pluses in (a) indicate the fit of the desorption data to Eq. (4) with $K_0=0$; the solid line in (a) indicates the background determined by the fit.

initial value; the signal returned to its background value in less than 600 s. Due to cryopumping in the vicinity of the sample, the effective pressure at the sample is expected to drop even more quickly in the low-temperature experiments.

The background counts before the gas was turned on are due primarily to ESD from residual impurity as dis-

cussed in Ref. 10. The decay of the counts after the gas flux is stopped approaches an asymptotic background shown by a solid line in Fig. 1(a) that is determined by a fitting process to be described below. This background is higher than the initial background, apparently due to physisorbed molecules bound to defects on the surface; after the substrate is heated above 20 K the background returns to the original level.

A range of average current densities was used for similar adsorption-desorption runs. The sample holder and radiation shield were warmed to above 50 K between each data set. Each data set started from nominally the same HD or H_2 dose. Desorption data after subtracting the fitted background and normalizing to the value at the start of the desorption are shown on semilogarithmic plots in Fig. 2. Except for the lowest current HD data in Fig. 2(a), the desorption data are clearly nonexponential. The dotted lines show fits to a model explained below which takes into account the nonuniform electron-beam profile.

TOTAL ESD REMOVAL CROSS SECTION: GENERAL CASE

When diffusion on the length scale of the electron-beam profile can be neglected,¹⁴ three processes contribute to any change in coverage: adsorption from any incoming flux F of molecules per unit area per unit time, ESD, and residual desorption not due to electrons. As discussed elsewhere,¹⁵ normal thermal desorption is extremely small for H_2 , HD, and D_2 monolayers at $T < 9$ K; the observed residual desorption is believed to be caused by infrared radiation from the room-temperature apparatus. In the coverage regime studied here, the dominant coverage loss will be from the commensurate solid islands which coexist in equilibrium with low-density two-dimensional vapor. When these islands are sufficiently large, edge effects will be small and the majority of desorption will be from the interior of the island. In this case the residual desorption rate constant K_0 , the total effective cross section for producing positive ions which escape the surface σ_p , and the total ESD cross section from removal of molecules from the surface σ ,

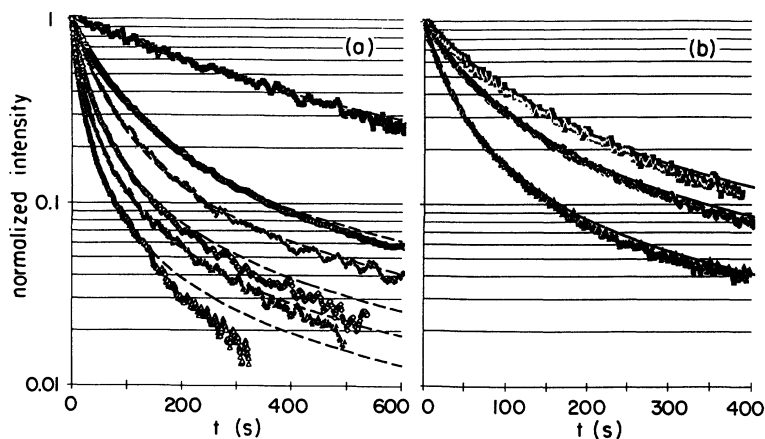


FIG. 2. Semilogarithmic plot of desorption data after subtracting the fitted background and normalizing to the value at the start of the desorption. The data at later times have been averaged to reduce statistical noise due to lower counts. The lines show fits to Eq. (4) with $K_0=0$. (a) Data for HD with J_0 in $\mu A/cm^2$ increasing from top to bottom: 0.037, 0.22, 0.43, 0.77, 1.23, and 1.50. (b) Data for H_2 with J_0 in $\mu A/cm^2$ increasing from top to bottom: 0.035, 0.069, and 0.17.

should be independent of coverage θ in molecules per unit area. Then the change in coverage with time is given locally by

$$d\theta/dt = sF - \sigma_i J_e(r)\theta - K_0\theta, \quad (2)$$

where s is the sticking coefficient, which may vary with coverage, and J_e is the current density from Eq. (1) in electrons per second per unit area.

The effective positive-ion cross section σ_p estimated in Ref. 10 is less than 10^{-5} of the total-removal cross section σ_t measured below. The number $P(t)$ of positive ions per unit time that reach the detector can be related to the coverage on the surface within the area sampled by the electron beam by

$$P(t) = P_b + \int dA \gamma \sigma_p J_e(r)\theta(r,t), \quad (3)$$

where P_b is the background ion signal, γ is the efficiency of detection which can depend on the ion mass and energy distribution, and the integration is over the surface area exposed to the detector.

TOTAL ESD REMOVAL CROSS SECTION: GAUSSIAN ELECTRON BEAM

Due to the spatial variation of $J_e(r)$, the coverage will vary over the region of the surface probed by the electron beam. Because our graphite samples are not much larger than the electron beam size at 62-eV energy, we do not have the option of rastering the electron beam to minimize the spatial variation of coverage. If the incident flux F is reduced to zero at $t=0$, if the coverage distribution is uniform at $t=0$ with $\theta(r,t=0)=\theta_0$, and if the substrate radius R is much larger than the Gaussian half-width of the beam [Eq. (1)], Eqs. (2) and (3) can be integrated to give a simple function

$$P - P_b = P_0 \exp(-tK_0) [1 - \exp(-t/\tau)] / (t/\tau), \quad (4)$$

where $P_0 = P(t=0) - P_b = \gamma \sigma_p \theta_0 I$ is the initial count rate above background, I is the number of electrons per second, and $(1/\tau) = J_0 \sigma_t$ is the rate constant for the ESD process.¹⁶ Because the ESD effect was much larger than the residual desorption for the current densities used here, K_0 was set to zero and the data were fit using three adjustable parameters, P_b , P_0 , and $1/\tau$. The total ESD removal cross section σ_t was then determined from a plot of $1/\tau$ vs J_0 .

To understand the large effects on the time dependence of ESD produced by a Gaussian beam profile, consider the case where the residual desorption can be neglected ($K_0=0$) compared to the ESD effect. Figure 3 shows the coverage spatial profile at several times in units of τ , superimposed on the electron-beam spatial profile. At $t=0$ (not shown) the coverage is uniform and the integral in Eq. (3) gets most of its contribution from the center of the beam. As the ESD erodes away the coverage in the center fastest, the remaining ion signal comes mainly from an annular region around the center with an effective radius increasing in time. If the beam were perfectly Gaussian, the signal $(P - P_b)/P_0$ would decay as

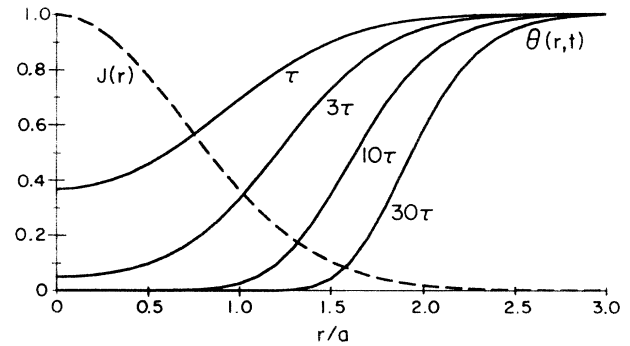


FIG. 3. Coverage profiles (solid lines) resulting from a constant removal cross section superimposed on the Gaussian electron current density profile (dashed line). The solid lines from left to right are at $t/\tau=1, 3, 10,$ and 30 . The radius r from the center of the beam is measured in units of "a", the width parameter of the Gaussian current density profile defined by Eq. (1).

$1/t$ for times such that $t > 4\tau$. However, any deviation of the edge of the spatial profile from a Gaussian or a slow variation in the background will show up more prominently at such long times and produce a deviation from Eq. (4).

TOTAL ESD REMOVAL CROSS SECTION: HD AND H₂ FOR 62 eV ELECTRONS

The dashed lines in Figs. 2(a) and 2(b) and the plusses in Fig. 1(a) indicate fits to Eq. (4). The small periodic

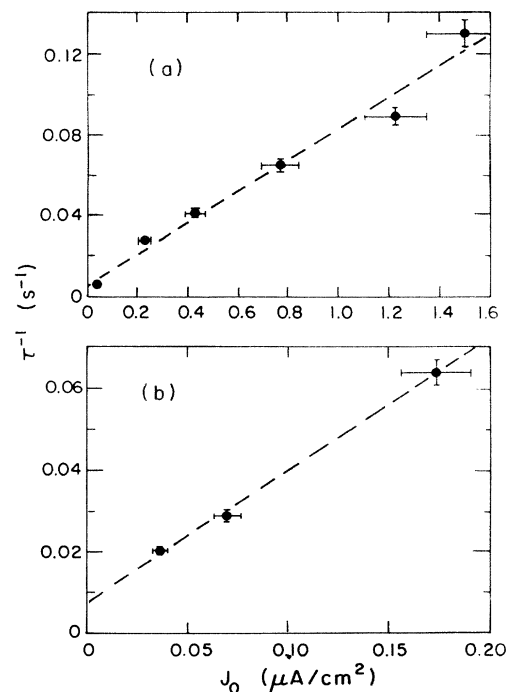


FIG. 4. Parameter $1/\tau$ deduced from fits to desorption data shown in Fig. 2 for a range of current densities. (a) HD, and (b) H₂. The slope of the dashed lines gives a total-removal cross section σ_t of approximately 1.2 nm^2 for HD and 5.2 nm^2 for H₂ for the 62-eV electrons used.

fluctuations visible in the data in the semilogarithmic plots of Figs. 2(a) and 2(b) could be due to small fluctuations in the sensitivity of the counting system; such fluctuations were not observed in measurements of the electron current. Systematic deviations from the fits visible in Figs. 2(a) and 2(b) at longer times can be due to deviations of the electron-beam profile edges from a Gaussian or from variations in background. Figure 4 shows the parameters $1/\tau$ from fits to Eq. (4) as a function of current density J_0 . The slopes obtained from Fig. 4 give ESD total-removal cross sections from HD (H_2) of approximately 1.2 (5.2) nm^2 for 62-eV electrons.¹⁷ The most significant source of error in the total-removal cross section determination is believed to be the uncertainty in the effective current densities J_0 . The uncertainties in J_0 shown in Fig. 4 lead to $\pm 20\%$ uncertainty in the cross sections.

The fact that the total desorption cross section σ_t is so much larger than the 0.01-nm² total-gas-phase-ionization cross section¹² at 62 eV suggests that the dominant process leading to desorption from the surface is different from processes starting with ionization such as those hypothesized for ESD of physisorbed Ar, Kr, and Xe.^{1-3,6} The larger removal cross section for H_2 compared to HD may be due to the weaker binding of H_2 due to increased zero-point energy. The binding energy of HD (H_2) in a commensurate monolayer on graphite is calculated to be 47 (44) meV.¹⁸ The out-of-plane acoustic-phonon density of states of the graphite surface layer extends up to about 58 meV.¹⁹ Nonequilibrium phonons excited directly by

the electron beam or indirectly by decay of electron-hole pairs and/or plasmons created by the electron beam may contribute to the large removal cross section. Such a coupling between the electron beam and the graphite phonons is clearly evidenced by observation of graphite phonons in electron-energy-loss measurements off the specular direction using 20-eV electrons.¹⁹ Beside the impact scattering regime which involves direct incident electron interaction with the phonon excitations, electron-hole pairs created by the electron beam can decay incoherently to give graphite phonons. At this time we are not aware of sufficient data on the electron-hole to phonon coupling to permit a quantitative estimate of the proposed effect. Future measurement of the total desorption yield versus electron energy may be able to provide a more definitive test of the proposed mechanism. Nonequilibrium phonons are also thought to be important in the infrared induced desorption of H_2 , HD, and D_2 from graphite¹⁵ and of HD from LiF.²⁰

ACKNOWLEDGMENTS

In addition to the acknowledgments in Ref. 10, we thank D. Menzel and R. Gomer for pointing out the study of Lin and Gomer on nonuniform electron current effects on ESD, M. B. Webb for helpful discussions, and A. Szabo for comments on possible tests of the phonon desorption hypothesis. This work was supported by NSF Grant No. DMR-91-19701.

*Author to whom all correspondence should be addressed.

Electronic address: fain@phys.washington.edu

¹E. Moog, J. Unguris, and M. B. Webb, *Surf. Sci.* **134**, 849 (1983).

²Q.-J. Zhang and R. Gomer, *Surf. Sci.* **109**, 567 (1981).

³Q.-J. Zhang, R. Gomer, and D. R. Bowman, *Surf. Sci.* **129**, 535 (1983).

⁴J. C. Lin and R. Gomer, *Surf. Sci.* **172**, 183 (1986). Lin and Gomer show that the nonexponential decay reported for Kr on W(110) in Ref. 3 was an artifact of nonuniform electron current density.

⁵P. Feulner, D. Menzel, H. J. Kreuzer, and Z. W. Gortel, *Phys. Rev. Lett.* **53**, 671 (1984).

⁶E. Steinacker and P. Feulner, *Phys. Rev. B* **40**, 11 348 (1989); E. Hudel, E. Steinacker, and P. Feulner, *ibid.* **44**, 8972 (1991).

⁷C. Leung and R. Gomer, *Surf. Sci.* **59**, 638 (1976).

⁸P. R. Antoniewicz, *Phys. Rev. B* **21**, 3811 (1980).

⁹Z. Gortel and A. Wierzbicki, *Phys. Rev. B* **43**, 7847 (1991).

¹⁰S. C. Fain, Jr., Bin Xia, and J. Peidle, preceding paper, *Phys. Rev. B* **50**, 14 565 (1994).

¹¹H. Wiechert, *Physica B* **169**, 144 (1991).

¹²D. Rapp, P. Englander-Golden, and D. D. Briglia, *J. Chem. Phys.* **42**, 4081 (1965).

¹³S. Andersson, L. Wilzen, M. Perrson, and J. Harris, *Phys. Rev. B* **40**, 8146 (1989).

¹⁴Bin Xia and S. C. Fain, Jr. (unpublished); measurements at

higher electron energies where the electron beam width is smaller can be used to place an upper limit on this diffusion.

¹⁵W. Liu and S. C. Fain, Jr., *J. Vac. Sci. Technol. A* **10**, 2231 (1992). In this paper, the residual desorption was assumed to be zero order for simplicity; the data were not complete enough to distinguish between zero- and first-order desorption and were not corrected for possible ESD effects.

¹⁶For simplicity, the analysis given assumes the electron beam is on continuously; as mentioned earlier the average current was varied in the experiment by changing the fraction of time (duty cycle) the electron gun was on, by either changing the length of the pulses (for HD) or changing the repetition rate of the pulses (for H_2). It can be shown that the result holds for this situation if the time average current is used.

¹⁷Preliminary ESD measurements using low-energy electron diffraction did not take into account the spatial nonuniformity of coverage produced by ESD at large electron fluences: B. Xia, W. Liu, and S. C. Fain, Jr., *Bull. Am. Phys. Soc.* **38**, 649 (1992); W. Liu, Ph.D. dissertation, 1992.

¹⁸A. D. Novaco, *Phys. Rev. B* **46**, 8178 (1992).

¹⁹C. Oshima, T. Aizawa, R. Souda, Y. Ishizawa, and Y. Sumiyoshi, *Solid State Commun.* **65**, 1601 (1988); T. Aizawa, R. Souda, S. Otani, Y. Ishizawa, and C. Oshima, *Phys. Rev. B* **42**, 11 469 (1990); T. Aizawa (private communication).

²⁰P. M. Ferm and G. M. McClelland, *J. Chem. Phys.* **98**, 700 (1993).